Distorted local environment around Zn on Cu(2) sites in $YBa_2Cu_3O_7$: An x-ray-absorption study

Frank Bridges and Guoguang Li
Physics Department, University of California, Santa Cruz, Santa Cruz, California 95064

James B. Boyce
Xerox Palo Alto Research Center, 3333 Coyote Hill Road, Palo Alto, California 94304

Tord Claeson
Chalmers Institute of Technology, Gothenburg, Sweden
(Received 19 November 1992; revised manuscript received 12 March 1993)

The substitution of Zn for Cu in $YBa_2Cu_3O_{7-\delta}$ (YBCO) causes a surprisingly large suppression of the superconducting transition temperature. However, there has been some controversy as to whether Zn replaces Cu in the CuO_2 plane sites, Cu(2), in the CuO chain sites, Cu(1), or in both sites. We present x-ray-absorption fine-structure (XAFS) data for samples from four different sources with several concentrations of Zn. Our data indicate that, in many samples, much of the Zn resides in ZnO (or ZnO-like) clusters; for some of these samples we have estimated the amount of ZnO present from our XAFS data. One group of samples showed no evidence for ZnO-like precipitates, indicating that in this case, most of the Zn is in solution, or in a YBCO-like environment. For this data Zn has about five nearest O neighbors at approximately equal distances of 2.03 Å. Furthermore, the distances to the Zn further neighbors are well defined, with little broadening. Our analysis indicates that Zn primarily occupies the Cu(2) plane sites, in contrast to Co and Fe, which reside in the chain sites. However, its local environment is significantly distorted; the Zn(2) atoms are displaced along the c axis toward the Cu(1) sites by about 0.2 Å. It is not clear whether the Zn atoms are uniformly distributed, or whether the observed distortion signifies some type of clustering; however, the sharpness of the transition supports a uniform distribution. Our work illustrates further the general tendency of $YBa_2Cu_3O_7$ to distort easily when slightly modified.

I. INTRODUCTION

The substitution[1–4] of other metal atoms for the constituent elements in ceramic, high-temperature superconductors, such as $YBa_2Cu_3O_{7-\delta}$ (YBCO or 1:2:3), is an important means of probing the parameters essential to superconductivity. This is especially true for Cu substitutions, as Cu plays a dominant role in these materials.[1–26] Substituting for Cu with trivalent magnetic atoms, such as Fe or Co, the divalent magnetic atom Ni, or the nonmagnetic atom Zn, as well as depleting the oxygen content in pure YBCO material,[27] all suppress superconductivity. On the other hand, replacing Y with rare-earth elements or Ba with alkaline earths usually does not affect superconductivity[4] very much (with some exceptions).

Cu and O form layered regions in the 1:2:3 compounds: the CuO_2 planes, in which each Cu(2) atom is surrounded by four oxygen atoms in the plane and one oxygen atom in an apical position, and the CuO chains, in which each Cu(1) atom has two O neighbors along the b axis and two neighbors along the c axis. Electrical transport occurs primarily within the CuO_2 planes, while the CuO chains are thought to be important as suppliers of charge carriers. The apical oxygen atoms O(4) that provide a bridge between the CuO_2 planes and the CuO chains appear to be important for charge transfer. Substitutions for Cu can go into both sites, or preferentially into either the chain or plane site. Since the site locations may affect the superconducting or normal-state properties in different ways, the investigation of substituted YBCO should help elucidate the roles of the chains and planes for superconductivity. In Fig. 1, we show the structure[27] of YBCO, including the various site definitions that we will use.

Zn suppresses the superconducting transition temperature T_c of YBCO more than any other dopant, even more than magnetic elements, the traditional pair breakers. However, the T_c suppression reported in the literature varies widely.[3–35] Many investigations indicate a nearly linear decrease of T_c with Zn concentration,[9,12,13,21,23,24,30,35] with T_c going to zero at 7–10 % Zn. A nonlinear dependence reported by some investigators[1,10,14,20,36] may be due to ZnO (or a Zn-rich compound) precipitates in the higher Zn concentration samples. A very strong suppression of T_c with Zn concentration is also found for the 1:2:4 variant of YBCO, with T_c going to zero with only 3.7% Zn.[37,38]

Despite many studies, there is still some disagreement on the substitutional site of Zn. This could be due to the presence of other phases, but it may be a real sample-preparation-dependent effect. It has, for example, been proposed that Co and Fe [normally on the Cu(1) site] can be moved to the Cu(2) site by appropriate sample treatment,[39,40] although our studies of Co-substituted materials do not support this claim.[41] Most studies indicate that Zn substitutes on the Cu(2)

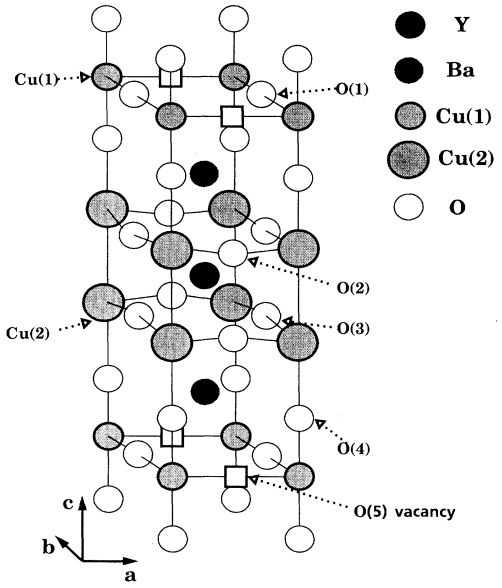

FIG. 1. The structure of $YBa_2Cu_3O_{7-\delta}$ for $\delta=0$, the fully oxygenated case (see Ref. 27). In the ideal case, the O(5) sites are vacant. For $\delta=1$, the O(1) are also fully depleted and the a and b axes are equivalent.

site,[1,3,14,20–24,30,32,34,35,42–46] but many of the arguments are indirect, i.e., based on the assumption that a strong depression of T_c must be connected to disturbances of the conducting CuO_2 planes, or that a physical property has a different parameter dependence for Zn than for Co or Fe substitutions which are known to go into the Cu(1) sites. For example, the diffusion of tracer elements is high for Cu, Ni, and Zn in YBCO, but substantially lower for Co, particularly along the c axis.[47] Shifts or the lack of shifts of Raman modes have also been used to determine the substitution site. In contrast to the situation for Co and Fe, the relatively pronounced 500-cm^{-1} mode, ascribed to the apical O(4) vibrations around Cu(1) (along the c axis), is not shifted by Zn or Ni substitution.[14,22] This has been taken as proof that Zn does not occupy the Cu(1) site. However, the change of distances from other atoms can also influence the Raman modes and hence this is not a direct proof of Cu(2) substitution. Similarly, the softening of the 291-cm^{-1} mode with temperature, in far-infrared reflection measurements, becomes more pronounced with Zn substitution.[48] The softening shows a maximum at 1% Zn; at higher concentrations, it decreases and returns to the value for pure YBCO at 3–5 % Zn. This softening is attributed mainly to transverse vibrations of oxygen atoms in the CuO_2 planes, and has been taken as an indication of a Cu(2) substitution.

A standard Ritveld analysis of neutron-diffraction data also supports a Cu(2) substitution site for Zn. Unfortunately, however, the scattering cross sections of Cu and Zn are not widely different, and the neutron data are not very sensitive to Zn. Considering only reflections that depend on the substitution site, it was concluded that Zn goes primarily into the Cu(2) site,[17] with possibly 10–20 % into Cu(1) sites. However, another group[8] has concluded from their neutron-diffraction data that Zn is preferentially in the Cu(1) site. The diffraction experiments are based upon long-range order and hence are less sensitive to local disorder than the x-ray-absorption fine-structure (XAFS) results reported here.

Some other work also favors Cu(1) as the site of Zn substitution.[8,13,36] The arguments are based mainly on expected changes in magnetic properties. There is an antiferromagnetic coupling between Cu atoms in the CuO_2 planes, leading to antiferromagnetic ordering in the insulating state of oxygen-deficient YBCO at low temperatures. Susceptibility and NMR experiments in such samples show that there is no change in this antiferromagnetic order (or the CuO_2 sheets) with Zn substitution. This would not be expected if the unfilled d-shell Cu(2) atoms were replaced by nonmagnetic Zn atoms, and hence it was concluded that Zn has to go into Cu(1) sites. Later NMR measurements on metallic, high oxygen content samples showed, however, an unusual Curie contribution to the ^{89}Y NMR width.[42] It was concluded that local magnetic moments in the CuO_2 planes are associated with the disorder induced by a fraction of Zn substituting on Cu(2) sites.[49] Nuclear quadrupole resonance[29,30,43] (NQR) and muon spin resonance[45] (μSR) experiments also indicate Zn substitution on the plane sites.

Some NMR experiments suggest the presence of a gapless state in Zn-doped YBCO.[43] In these experiments, it is found that the relaxation time obeys the Korringa relationship, $T_1T=$const, which is characteristic of free electrons at the Fermi surface. The gapless state has also been indicated by specific-heat[16,50] and point-contact tunneling measurements.[51] Some magnetic measurements suggest that the superconducting fraction is small for the Zn-doped samples. In one study,[31] increasing hydrostatic pressure leads to an anomalously large increase in T_c for 5% Zn in YBCO compared to pure YBCO. However, it is important to recognize that this result is for samples with an inhomogeneous Zn distribution as evidenced by a broad width to the superconductive transition.[31] In another study, on samples with a sharp transition, no pressure dependence of T_c is observed up to 4% Zn.[28]

The broad transition width and anomalously large increase in T_c with pressure for some YBCO:Zn samples has led to another proposal in which the possibility of a nonuniform spatial distribution of Zn atoms plays a dominant role. Phillips[52–55] has introduced a microdomain model where domains of stoichiometric YBCO with thickness $d>100$ Å, but $d\ll 2000$ Å (the typical separation between twin boundaries) are separated by domain walls with a high Zn concentration and depressed superconductivity. The walls have a thickness w with w/d typically of order 0.1. The buckling of the planes is expected to be exaggerated in the domain region because Zn usually prefers a fourfold coordination with O. As Zn is dissolved, it segregates to the domain walls up to a critical bulk composition of $x_0=0.01$ (corresponding to $x=0.1$ in the wall region, the limit of solubility). Above this concentration, Phillips suggests that a phase segregation begins on a microscopic scale with increasing lattice distortion and domain-wall thickness. The model is claimed to explain a number of observations: the phonon

softening of the far-infrared modes,[48] the residual normal-state specific heat,[16,50] the large pressure dependence of T_c for the nonuniformly doped YBCO:Zn samples,[31] and the multigaps found in tunneling curves.[51]

Our experiment utilizes XAFS (x-ray-absorption fine structure) to study the local structure of substituted YBCO. In particular, the Zn K-edge absorption data provides information about the distances to, the number of, and the kinds of neighbors in surrounding shells about the Zn atom. These distributions can be compared with different models. We will show that when there is no substantial precipitation of ZnO, the Zn atoms substitute for Cu, but not at the Cu(1) site. If they go into Cu(2) sites, the environment has to be distorted. A preliminary report has been given earlier.[56]

The distortion about the Zn atom which we present here is quite distinct[25,41] from that for Co and Fe. Although the nearest-neighbor bond length is increased by nearly 0.1 Å, the second-, third-, and fourth-neighbor distances are well defined, with relatively little broadening (little disorder). Consequently, in contrast to the case for Co and Fe dopants,[25,41] the multipeak in the Zn XAFS r-space data corresponding to these further neighbors is large, comparable in amplitude to that for pure YBCO.

Our samples were obtained from several sources. In Sec. II, we briefly describe these materials, their preparation, and the x-ray measurements. Section III describes our data reduction method, while in Sec. IV we present the data in both k and r space. Section V discusses the detailed fit of the data to a sum of standards. Finally, we compare our results with other experiments and discuss their implications in Sec. VI.

II. SAMPLES AND MEASUREMENTS

We have investigated the XAFS on the Cu K edge (8980 eV) and on the Zn K edge (9660 eV) for a number of $YBa_2(Cu_{1-x}Zn_x)_3O_{7-\delta}$ samples with differing Zn concentrations x, from 0.05 to 0.10. The materials were obtained from four sources. An early set of measurements was made on a series of samples prepared by Tarascon[1] at Bellcore using standard sintering techniques with multiple grinding and resintering. Later measurements were performed with sintered samples from the Karlsruhe group in Germany[8] and two sets of samples, prepared by sintering and by the sol-gel technique,[26] from Chalmers in Sweden. The XAFS data show that some of the samples contained ZnO particles, and will be discussed below. Several of the Chalmers samples had been used about a year earlier for other types of experiments, and at that time showed no sign of impurity phases. However, new Raman measurements[57] on one of these old samples did show traces of a segregated phase, suggesting a slow degradation of the samples with time. The samples with the least amount of ZnO phase were those from Karlsruhe. The detailed analyses and results, presented in this paper, were carried out on these samples. Details about the Karlsruhe samples[8] are given in Table I. Some points to note are: (1) There is very little change of lattice constant with Zn concentration; (2) the superconducting transition is very sharp, indicating uniform Zn substitution; and (3) there is a small decrease in O content as the Zn concentration is increased. See Ref. 8 for more sample information.

For our XAFS experiment, the YBCO:Zn samples were first ground to a fine powder ($<30\mu$) and then brushed onto Scotch tape. Several layers, typically 3–4 double tape layers for the Cu and Zn edges, were stacked in order to obtain a sample with a thickness of approximately two absorption lengths. Each sample was selected to be free of pinholes; x-ray photographs were taken at the synchrotron to check for spatial uniformity. During the experiment, the samples were cooled to liquid-nitrogen temperature (about 80 K) in a cryostat with kapton windows. The temperature was measured with a thermocouple in contact with the sample holder. Reference samples of ZnO, Cu_2O, Cu, CuI, and RbBr were also prepared and investigated in a similar way.

The XAFS experiments were carried out on beamline 4-1 at the Stanford Synchrotron Radiation Laboratory using a Si(220) monochromator. In order to remove the harmonics of the desired photon wavelength, the Si crystals were detuned 40–50 % from maximum intensity. A leveling feedback system was used to control the piezoelectric crystal of the monochromator to keep the incident photon flux constant. The slit size in front of the sample was 0.7 mm (vertical)×5 mm (horizontal). The monochromator and the geometrical arrangement gave an energy resolution of about 1.5 eV at the Cu K edge. All absorption measurements were taken in the transmission mode using gas ionization counters containing N_2 gas. Simultaneously, a third counter measured the intensity transmitted through a reference foil of Cu or Zn to monitor possible shifts in energy of the monochromator.

TABLE I. Details about the Karlsruhe samples $YBa_2(Cu_{1-x}Zn_x)_3O_{7-\delta}$ used in the detailed XAFS analysis. The lattice constants were obtained from neutron data at 20 K. The oxygen content, determined from neutron-diffraction data and from iodometric titration, was identical within the error of ±0.05.

	Lattice constants			Inductive T_c		Resistive T_c		Oxygen
x%	a (Å)	b (Å)	c (Å)	T_c^{mid} (K)	ΔT_c (K)	T_c^{mid} (K)	ΔT_c (K)	content (±0.05)
5.0	3.817	3.888	11.642	36.4	1.5	39.2	3.7	6.95
7.5	3.819	3.890	11.640	17.3	2.0	25.0	5.8	6.93
10.0	2.823	3.891	11.649	0		0		6.89

III. DATA REDUCTION

To obtain quantitative estimates of the structural parameters, the absorption data must first be reduced to obtain the XAFS oscillations in k space. First, the slowly varying prethreshold background absorption was subtracted to yield the absorption due to the atom of interest. Next, the background above the edge was fit to a series of splines and the XAFS function $\chi(E)$ was determined. $\chi(E)=[\mu(E)-\mu_0(E)]/\mu_0(E)$, where the absorption cross section $\mu(E)$ includes both the absorption edge and the XAFS oscillations, and $\mu_0(E)$ is the free-atomic absorptance. Finally, the data were transformed to k space ($\hbar^2k^2/2m_e=E-E_0$, where E_0 is the energy at one half the absorption-edge height). The resulting XAFS function[58]

$$k\chi(k)=\Sigma_j\{N_jF_j(k)\sin[2kR_j+\phi_j(k)] \times\exp(-2k^2\sigma_j^2-2R_j/\lambda_j)\}/R_j^2$$

contains the desired structural parameters: distances R_j, number of neighbors N_j, and the broadening σ_j, as well as the XAFS response parameters—the phase shifts $\phi_j(k)$ (which depend on both the absorbing and backscattering atoms), the scattering amplitudes $F_j(k)$, and the electron mean free path λ_j.

Next, the XAFS in wave-vector (k) space is Fourier transformed to real (r) space, using as long a k interval as possible. The quality of the r-space data at low r is dependent on the fit of the background, particularly near E_0. We have developed a background subtraction technique which is discussed in more detail in a separate paper.[59] We first use an automated process to choose the value of $E_{\min}$, the lowest energy of the background fit, to obtain a monotonic decease in the overall amplitude of the r-space data at low r (typically below 1 Å). From a fit of the first two neighbors of this data to theoretical standards (obtained using the FEFF program developed by Rehr *et al.*[60]) we have an approximate measure of the amplitude, width, and position of the first two neighbor components. These components are then converted to energy space and subtracted from the original E-space data, resulting in absorption-edge data with most of the low-frequency XAFS oscillations removed (however, the high-frequency components remain). A new background is determined using a multiple spline or high-order polynomial fit to this modified data. The original data are then reduced using this new background.

A qualitative picture of the radial distribution of neighbors can then be obtained by inspecting the Fourier transforms of the XAFS oscillations. However, to obtain numerical values for R_j, N_j, and σ_j, we must perform least-squares fits of the real and imaginary parts of the Fourier transform of $k\chi(k)$ to a sum of standards. In these fits, we have generally used experimentally determined standards, extracted from low-temperature data for compounds with a well-defined nearest-neighbor environment, to account for the phase shifts $\phi_j(k)$ and the scattering amplitudes $F_j(k)$.

For the Zn edge, the situation is more complicated than for the Cu edge. There are background oscillations from the high-k part of the Cu K-edge XAFS which interfere with the Zn K-edge XAFS because the separation between the two edges is only 680 eV. For the low concentration YBCO:Zn samples investigated here, we find that the Cu K-edge XAFS signal is essentially the same as that of a good unsubstituted sample within the k space available for comparison. We have high-quality data out to $k=19$ Å^{-1} for the XAFS of an unsubstituted sample. We can therefore remove the remaining Cu K-edge XAFS in the region above the Zn K edge using this Cu data, following a procedure similar to that which we developed to subtract the Pb $L_{\rm III}$ XAFS contribution from Bi $L_{\rm III}$-edge data for Ba(Bi,Pb)O_3 samples.[61] In the preedge region below the Zn edge, we fit the Cu XAFS oscillations of the Zn-substituted sample to the Cu K-edge data of the pure, unsubstituted YBCO. This provided the correct amplitude of the Cu K-edge data for subtraction, and eliminated the need to estimate this factor from step heights or the need for additional fitting parameters in the fits to the Zn spectra.

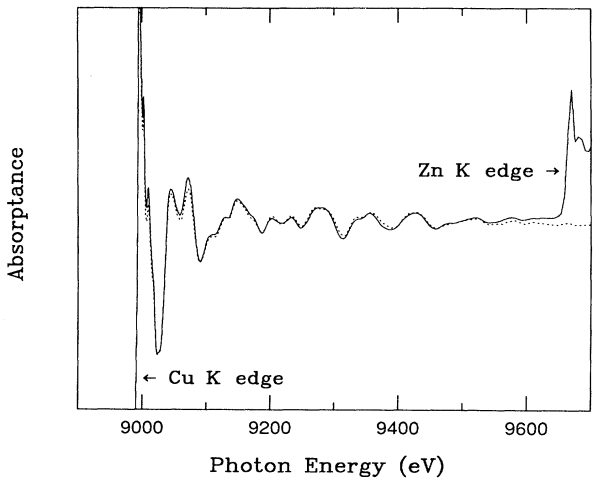

FIG. 2. The x-ray absorption below the Zn K edge. Note the presence of oscillations from the Cu K-edge XAFS. The dotted line shows the Cu K-edge absorption data of a pure YBCO sample; the amplitude of this trace has been adjusted to fit the Cu XAFS oscillations in the Zn-substituted sample. The background-corrected Zn data is obtained by subtracting this normalized Cu K-edge data from the Zn K-edge data.

In Fig. 2, we show the structure in the data for one of the $x=0.1$ samples below the Zn K edge. The dotted line shows the Cu K-edge data from a high-quality pure sample $YBa_2Cu_3O_{6.98}$, that have been normalized to fit the Cu XAFS in the Zn preedge data. The remaining Cu XAFS oscillations above the Zn edge are quite small, and are removed by subtracting this normalized Cu XAFS data from the Zn K-edge data.

IV. PRESENTATION OF DATA

The Zn k-space data, obtained after a standard reduction of the background-corrected data, are shown in Fig. 3 for $x=0.1$, 0.075, and 0.05. These XAFS spectra agree very well out to $k=13$ Å^{-1}, which means that the Zn

atoms reside in essentially the same environment for the three concentrations.

The Fourier transforms (FT) of $k\chi(k)$ at the Zn K edge for the three Zn-substituted samples are compared with the Cu K-edge, r-space XAFS of a pure sample in Fig. 4. Here we show the real part of the transform and the envelope function $\pm[(\mathrm{Im})^2+(\mathrm{Re})^2]^{1/2}$. Several points should be noted. First, the Zn K-edge, r-space XAFS for the three concentrations are nearly identical and they are, overall, roughly similar to the Cu K-edge XAFS. The equal amplitudes of the first-neighbor peak for the Zn atom in Figs. 4(a)–4(c) indicate that the background subtraction works very well. Second, the first-shell O peak for the Zn K-edge data is larger and shifted to higher r by nearly 0.1 Å compared to the Cu K-edge data. This was noted in earlier studies.[35] Third, the peak near 3.2 Å in the Cu K-edge r-space data, which arises from Y and Ba neighbors, is shifted down in r by about 0.15 Å. Fourth, an oscillation in the real part of the FT of the Cu K-edge data near 2.8 Å, which arises mainly from part of the Cu(2)-Y component, is not observed in the Zn K-edge data. Either it is missing or the Zn-Y component has moved to a slightly longer distance, making it indistinguishable from other neighbors without a detailed fit. Last, the real part of the FT in Fig. 4, from 3.6 to 3.9 Å, is almost the same for the Cu K-edge data of pure YBCO and for the Zn K edge of YBCO:Zn. This structure, which arises primarily from Cu/Zn neighbors, is broadened and shifted very slightly to larger r in the Zn K-edge data compared to the Cu K-edge data. These observations suggest that Zn substitutes for Cu but that the Zn site is distorted. The above qualitative features provide a set of starting parameters for the detailed fits discussed below.

To gain further qualitative insight into the distortions around the Zn atoms, in Fig. 5 we compare the r-space data with the corresponding K-edge data for Co and Ni dopants as well as pure YBCO. These data were collected under similar experimental conditions. First, consider the nearest-neighbor O shell, which occurs between 1.1 and 2.1 Å. We have added a vertical line for reference, at the value of r corresponding to the peak of the real part of the Ft for the pure sample (bottom trace). For Ni, the corresponding peak is nearly at the same place. However, for Co, the main peak position is shortened by about 0.1 Å, while for Zn, it is lengthened by about 0.1 Å. The peak amplitude is somewhat decreased for Ni and Co K

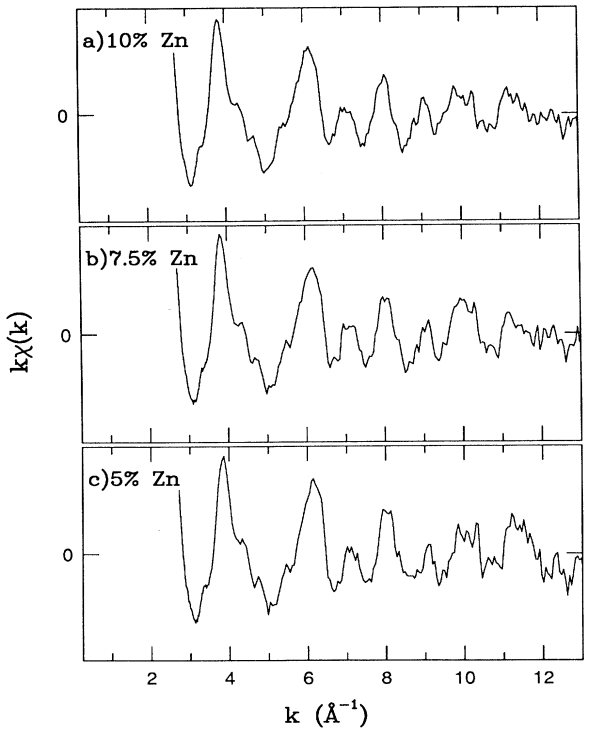

FIG. 3. The k-space XAFS data at the Zn edge (after subtracting the Cu background as described in the text) for 5%, 7.5%, and 10% Zn in $YBa_2Cu_3O_{7-\delta}$. The data were collected at 80 K.

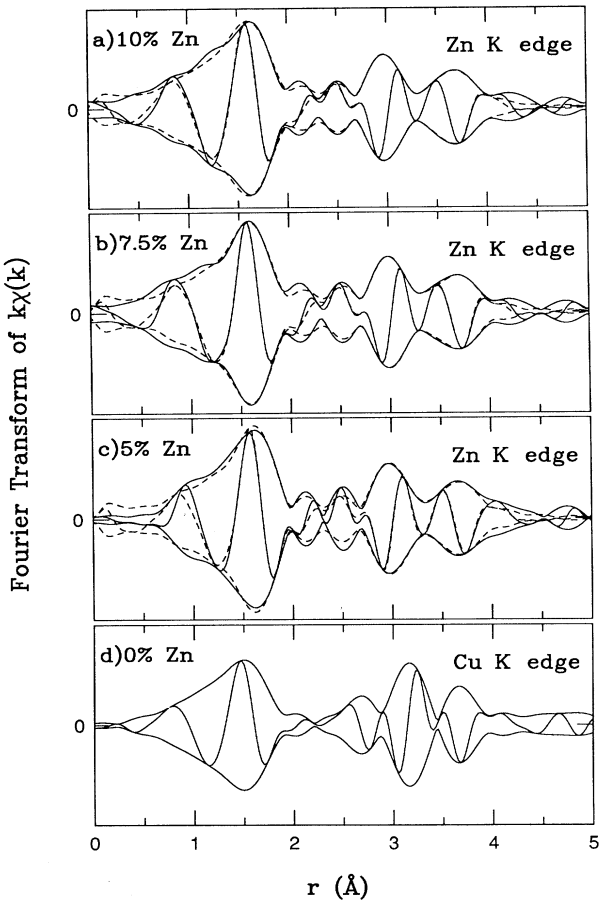

FIG. 4. (a)–(c) The r-space data for the traces in Fig. 3 obtained by a Fourier transform over the range 3.2–12.5 $Å^{-1}$, with a 0.3-$Å^{-1}$ Gaussian rounding of the window. (d) The bottom trace is the corresponding Cu K-edge data of a pure sample, provided for comparison. The fast oscillations are the real part of the FT and the envelope is $\pm\sqrt{(\mathrm{Im})^2+(\mathrm{Re})^2}$. The dotted lines represent fits to the data for each composition.

edges as compared to the Cu K edge; it is slightly larger for the Zn K edge.

In the multipeak region, from about 2.8 to 4.0 Å, which corresponds to the Y, Ba, and Cu (or impurity-atom) neighbor shells, the amplitude is considerably reduced for the Ni and Co K edges in substituted samples compared to the Cu K edge in the pure sample. For Ni, the peaks are slightly broadened, and strong destructive interference[27] between the Ni(1)-Ba and Ni(2)-Ba components produces a low amplitude near 3.2 Å. For Co-substituted samples, there is no Y neighbor for Co on a Cu(1) site, but several distinct Co-Ba and Co-Cu/Co distances[25,41,62] are needed to fit the data. This indicates an off-center displacement of the Co atom, probably along the ⟨110⟩ direction.

In contrast, the Zn K-edge data have a large amplitude in the multipeak region 2.8–4.0 Å, although the position of the largest peak (the Zn-Ba and Zn-Y contributions) is shifted to lower r. The large amplitude indicates that little broadening is present and that the number of distinct bond lengths must be small, i.e., that the lattice site of Zn must be rather well defined.

Many of the investigated samples have tiny particles of ZnO. In some cases, the amount of ZnO may be time dependent, as more recent Raman measurements[57] found traces of ZnO in samples that showed no zinc oxide a year earlier. However, the amount of ZnO observed in these Raman experiments is still small compared to the fraction of ZnO we have found in our XAFS studies. In Fig. 6, we compare the Zn K-edge, r-space data for four 10% Zn-substituted samples with that for ZnO. The major feature of the ZnO data is a large Zn-Zn peak in the FT from 2.8 to 3.0 Å, which corresponds to 12 Zn neighbors. If we now compare the ZnO data with the $YBa_2(Cu_{0.9}Zn_{0.1})_3O_{7-\delta}$ samples in the top four traces, we

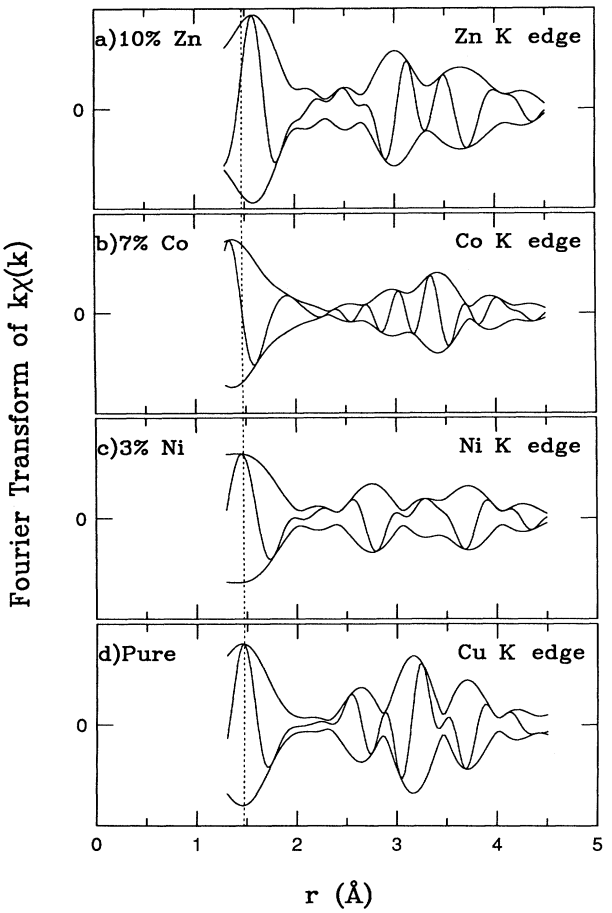

FIG. 5. A comparison of the r-space data of Zn-, Co-, and Ni-substituted $YBa_2Cu_3O_{7-\delta}$ with the Cu K-edge XAFS of a pure sample. The dotted line marks the peak in the real part of the Fourier transform for the oxygen peak of the pure sample. Note the shifts of the oxygen peaks and the change in the structure of the further-neighbor shells in the range of 2.5–4 Å. The FT range is 3.2–11.5 $Å^{-1}$.

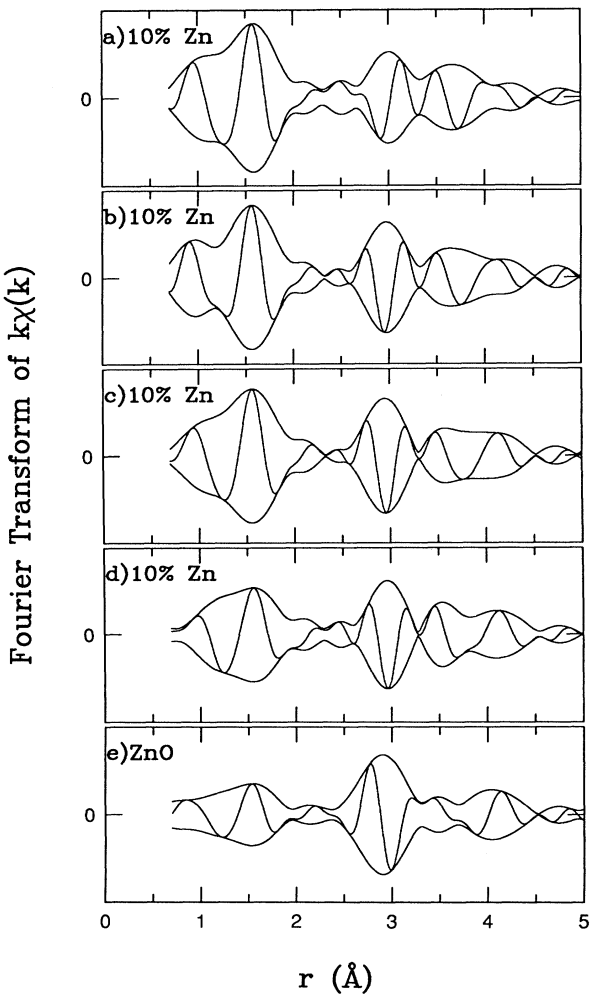

FIG. 6. A comparison of the r-space data for several 10% Zn samples containing ZnO-like particles, with ZnO [bottom trace, (e)] and with the Karlsruhe sample which is relatively free of ZnO [top trace, (a)]. (b) and (c) Traces for a solgel prepared and a sintered powder sample, originating from Chalmers. (d) The trace for a sintered powder sample from Tarascon. The vertical scale for the ZnO data is a factor of 2 larger than for the Zn-substituted YBCO samples. The FT range is 3.3–11.0 $Å^{-1}$, with a Gaussian window of 0.3 $Å^{-1}$.

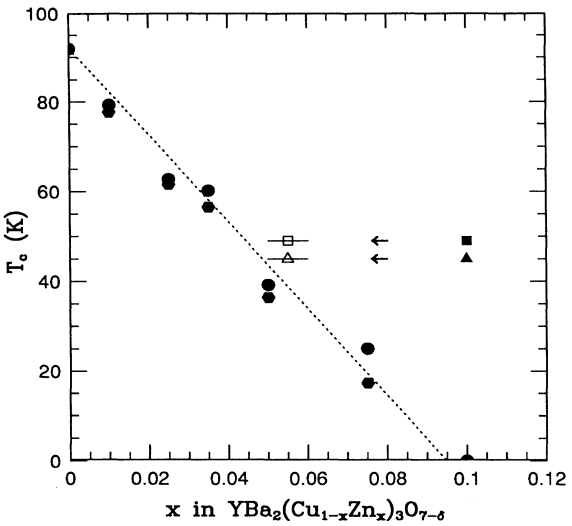

FIG. 7. A plot of T_c (midpoint) as a function of the Zn concentration for the Karlsruhe samples and two of the 10 at.% Zn samples containing ZnO. Solid circles–Karlsruhe resistive; solid hexagon–Karlsruhe inductive; solid square–Chalmers sintered; solid triangle–Tarascon; open square and triangle–Zn concentration corrected for ~45% of the Zn in the form of ZnO from our XAFS analysis. Note the greatly improved agreement with the other measurements.

see that the three middle traces show a strong resemblance to the Zn-Zn peak of ZnO in the range 2.8–3.0 Å (note particularly the real part of the FT shown in this figure), indicating a significant ZnO component. However, the top trace (the Karlsruhe sample) has little, if any, ZnO component. The amount of ZnO in a YBCO samples [Figs. 6(b)–6(d)] can be estimated from fits of these traces (over a wide range in r space, 1–4 Å) to a sum of ZnO and the top trace in Fig. 6 (which is assumed to have no ZnO present). For the spectra in which ZnO is clearly identified (in 10% Zn samples), the amount of Zn in a ZnO-like environment is in the range of 40–50 % for various samples. Assuming that the remaining Zn fraction is in solution in YBCO, we obtain an *upper* limit to the actual concentration of Zn dissolved in YBCO. Using this concentration, T_c decreases linearly with concentration x for these samples, as shown in Fig. 7. The large amount of ZnO found using XAFS together with the small amount visible using x-ray diffraction or Raman spectroscopy, indicate that the ZnO particles must be very small.

V. DETAILED EXTRACTION OF STRUCTURAL PARAMETERS

The two Cu sites in YBCO have distinctly different environments. Within a distance of 4 Å, Cu(1) has eight Ba neighbors, no Y neighbors, two O(4) neighbors at 1.86 Å, and two O(1) at about 1.94 Å. The Cu(2) site has four Y neighbors, four Ba neighbors, four planar oxygens O(2,3) at about 1.94 Å, and one longer O(4) bond at about 2.3 Å. The different neighbor separations are summarized in Table II.

In order to extract accurate estimates of the distances and numbers of different neighbors, we have to fit our data to a sum of well-defined standards. Since Cu and Zn are neighbors in the Periodic Table, we can utilize our Cu-O standard, extracted from the compound Cu_2O, to make a Zn-O standard. The Cu-O standard, which has a well-defined bond length of 1.85 Å, must be modified, using the FEFF theoretical calculations[60] to account for the different central-atom phase shifts from Cu ($Z=29$) to Zn ($Z=30$). For Zn-Y, we use a modified Rb-Br standard from RbBr, and for Zn-Ba, a modified Cu-I standard from CuI. For Zn-Cu and Zn-Zn we used a modified Cu-Cu standard, extracted from copper foil. The modified standards based on Cu-O and Cu-Cu were tested in a fit of the XAFS for ZnO. They gave the expected distribution of near neighbors for that case.

In our fits we started with parameters that correspond to particular assumptions about the substitution site. The ratios of amplitudes were constrained to correspond to the assumption under consideration [e.g., for Zn on the Cu(2) site, the amplitudes were constrained to correspond to equal numbers of Y and Ba atoms]. Distortions in the atomic positions were introduced that were self-consistent. For example, if the Zn(2) atom is displaced along the c axis, a lengthening of the Zn(2)-Y distance would require a corresponding shortening of the Zn(2)-Ba distance.

We first used a single Zn-O standard to fit the first-neighbor O shell around the Zn atom. For the $x=0.1$ sample, on which we concentrate our discussion, the main peak corresponds to about five neighbors, at a distance of about 2.02 Å. A series of fits using two and three Zn-O standards showed that there is no short bond length near 1.86 Å [expected for a Cu(1) site] and no long bond near 2.3 Å. The long Zn(2)-O bond length, expected for a Cu(2) site, is either close to that of the main peak (i.e., our fit for this assumption gives four neighbors near 2.01 and one at 2.05 Å) or shifted to a significantly higher

TABLE II. The separation and number of neighbors about each of the Cu sites in YBCO. The distances in the a-b plane have been averaged.

Cu-X Pair	No. Nbrs.	r (Å)
Cu(1)-O(4)	2	1.86
Cu(1)-O(1)	2	1.94
Cu(1)-Ba	8	3.47
Cu(1)-Cu(1)	4	3.85
Cu(2)-O(2)	4	1.94
Cu(2)-O(3)		
Cu(2)-O(4)	1	2.30
Cu(2)-O(2)	4	3.67
Cu(2)-O(3)		
Cu(2)-Y	4	3.20
Cu(2)-Ba	4	3.38
Cu(2)-Cu(2)	1	3.37
Cu(2)-Cu(2)	4	3.85

r (about 2.7 Å if we start our fit with a long distance).

We next included the contributions of Zn-Y, Zn-Ba, and Zn-(Cu/Zn) pairs in order to fit the peaks out to 4.0 Å. In these fits, we used starting parameters and constraints corresponding to particular assumptions about the substitution site. No reasonable fit was obtained for substitution on the Cu(1) site, even allowing the Zn(1) to be displaced significantly along the c axis. Note that displacements of Zn(1) in the a-b plane would result in several distinct Zn(1)-Ba and Zn(1)-(Cu/Zn) separations. The sum of these peaks at different distances would lead to destructive interference (as observed in YBCO:Co) and lead to a small XAFS multipeak in the $r=2-4$ Å region. This would be contrary to the experimental results, which show a large amplitude for the further-neighbor shells, comparable in amplitude to that of pure YBCO (see Fig. 4).

If we start with the assumption that Zn substitutes on the Cu(2) site, we must invoke a distortion of this site to obtain a good fit to the data. Such a distortion can be modeled by displacing the Zn(2) atom along the c axis toward the Cu(1) site by ~ 0.2 Å. This would give somewhat larger Zn(2)-[O(2)/O(3)] distances, shortened bonds of Zn(2)-O(4) and Zn(2)-Ba, and longer Zn(2)-Y and Zn(2)-[Cu(2)/Zn(2)] neighbor distances. We note that a distortion along the c axis retains the axial symmetry about the axis for each Zn atom. Existing bonds are lengthened or shortened but there are no additional bond lengths or a distribution of further-neighbor distances that would cause phase interference and lead to a decrease of the XAFS amplitude of the further neighbors. This is also in agreement with the observed data. The fits corresponding to a distorted Cu(2) site occupancy by Zn are shown as dotted lines in Fig. 4. The agreement between the data and the fits is very good, especially when the large range of the fit in r space is taken into account. The fit results are tabulated in Table III; the average nearest-neighbor Zn-O distance, the lengthened Zn-Y distance, and the shortened Zn-Ba distance are all consistent with a displacement of Zn by ~ 0.22 Å. However, the long Zn(2)-O bond that is 3.67 Å in pure YBCO, is 3.90 Å in YBCO:Zn, somewhat longer than the model prediction 3.84 Å. This suggests that the distortions of the O within the Cu(2)O planes has also changed. (The planar Zn-[Cu(2)/Zn(2)] component has a large amplitude and is longer (4.04 Å) than expected, in part because of forward scattering through the intervening O atom.)

At the 10% Zn level, one needs to consider possible interactions between Zn atoms or clustering effects. In XAFS, we cannot distinguish between a Zn or a Cu backscattering atom because Zn and Cu are neighbors in the Periodic Table. Only indirect arguments may be applied. However, we emphasize that for the 5%, 7.5%, and 10% Zn samples, the local environment is identical within our estimated errors, and the broadening of the Zn(2) further-neighbor distances about the c axis are small. Consequently, we have no evidence for or against clustering of Zn atoms within the plane; if clustering occurs, it does not change the lattice parameter significantly. It might be possible that Zn(2) atoms are paired up along the c axis, as the distortions found in our analysis are not very sensitive to such a pairing. However, we note that the narrow width of the superconducting transition in our samples suggests a uniform distribution of Zn.

A summary of the different Zn(2)-neighbor-atom distances that gave the best fits to our Zn XAFS data, is given in Table III. Note that the results for all concentrations are essentially the same. A small amount of Zn on the Cu(1) site cannot be excluded but it is likely $< 10\%$, if present at all in the Karlsruhe samples.

VI. DISCUSSION OF RESULTS

Our analysis of the Zn K-edge XAFS data indicates that the substitution of Zn occurs primarily on distorted Zn(2) sites, with the Zn(2) atom displaced along the c axis toward the Cu(1) site. However, moving only the Zn atom may not be very physical, and small displacements of the Zn neighbors relative to the rest of the unit cell are likely to be present. In YBCO, there is a buckling of the CuO_2 planes by movements of the O atoms in the c direction. According to the microdomain model,[52–55] the distortions would be even stronger in the domain-wall regions. It has been suggested that the addition of Zn might increase the tendency for domain-wall formation, because Zn prefers a tetrahedral environment (as is found in ZnO, where each Zn atom is surrounded by a somewhat distorted tetrahedron of O atoms). A modification of the oxygen buckling, with two of the O(2)/O(3) atoms moving toward the Cu(1) site, might cause a semi-

TABLE III. The number of neighbors and Zn-X distances about the Zn site in YBCO, obtained from the XAFS analysis. The model results for a displacement of Zn toward Cu(1) by 0.22 Å, with the assumption that the rest of the crystal is not distorted, are also included. The fit results for the planar Zn(2)-Cu(2) are enclosed in parentheses; r is too long and the amplitude is too large because forward (multiple-path) scattering has not been included. Errors: r, ±0.02 Å; Nbrs. ±10%.

	5% Zn		7.5% Zn		10% Zn		Model
Zn-X pair	Nbrs.	r (Å)	Nbrs.	r (Å)	Nbrs.	r (Å)	r (Å), (Nbrs.)
Zn(2)-O	5.2	2.03	5.0	2.02	5.3	2.03	1.99(4);2.07(1)
Zn(2)-O	4.2	3.90	4	3.90	4.2	3.93	3.84(4)
Zn(2)-Y	4.3	3.33	4.2	3.32	4.1	3.33	3.32(4)
Zn(2)-Ba	4.3	3.25	4.2	3.26	4.1	3.25	3.25(4)
Zn(2)-Cu(2)	1.1	3.60	1.1	3.57	1.0	3.6	3.58(1)
Zn(2)-Cu(2)	(6.5)	(4.04)	(6.5)	(4.04)	(6.5)	(4.04)	3.87(4)

tetrahedral environment, particularly if there were an O(4) vacancy. However, our data for the three different concentrations *does not support* such a hypothesis. Although our samples have a small *decrease* in O content with increasing Zn concentration, we find a *larger* amplitude for the Zn-O nearest-neighbor peak, with 5–5.5 neighbors. Our finding that zinc occupies a distorted Cu(2) environment might be taken as a support of a microdomain model, but not because of a tendency to have fourfold symmetry. Our conclusion that the Zn atoms reside in a well-defined site, in which the main YBCO symmetry is retained [but with the Zn(2) atoms displaced along the c axis] argues against such a domain-wall model.

Another possible indication of a small-scale inhomogeneity model might be the varying degree of ZnO-like precipitates that we find in some sources of the samples, which are not easily seen using other techniques. However, the fraction of Zn in ZnO precipitates clearly depends on the samples preparation, and such inhomogeneity is not an inherent property of the YBCO:Zn system.

A crucial consideration from the standpoint of superconductivity is why and how Zn suppresses T_c. Some have suggested a break in the magnetic coupling as a result of replacing a spin-$\frac{1}{2}$ copper atom by a spin-0 Zn atom. However, several studies indicate that there is only a small correlation between superconductivity and the magnetic properties for Zn impurities. T_c is strongly dependent on the concentration of holes in the CuO_2 planes, which in turn can easily be modified by structural changes that either partially localize holes on some Zn-O or nearby Cu-O bonds, or modify the charge transfer from the polarizable Ba-O(4) layer or the Cu(1) chains through the apical O(4) atoms. There is a strong correlation between T_c and changes in the Cu-O vibrations observed in Raman measurements. Our XAFS measurements indicate a strong modification of these bonds [i.e., Zn(2)-O bonds] when Zn replaces Cu(2). These modifications may account, through the charge-transfer model, for the strong suppression of T_c via Zn substitution.

VII. CONCLUSION

It was possible to remove the background oscillations of the high-k, Cu K-edge XAFS to obtain high-quality Zn K-edge XAFS data for dilute Zn in YBCO. Our analysis of both the O and further-neighbors peaks is inconsistent with Zn substituting primarily on the Cu(1) chain sites. A structure that fits the data has the Zn on a Cu(2) site in the CuO_2 plane, in a distorted (but not disordered) environment. This can be achieved by a displacement of the Zn(2) toward the Cu(1) atom by ~ 0.2 Å. A more complex model with a clustering of Zn in domain walls cannot be excluded, but appears unlikely in view of the fact that the Zn(2) environment is the same in each sample investigated. In addition, the narrow width of the superconductive transition in these samples suggests a uniform Zn distribution,[28] contrary to the domain-wall model in which Zn is concentrated in the wall region.

This work illustrates further the tendency of $YBa_2Cu_3O_7$ to distort easily when substituted. Each of the modifications that we have studied, O removal, Co, Fe, Ni, and Zn substitutions, have all resulted in a significant distortion of some part of the unit cell. This "softness" of parts of the unit cell, which may also be connected with a movement of the O(4) bridging oxygen, may play an important role in the superconductivity by controlling charge transfer between layers or by localizing holes (or electrons).

ACKNOWLEDGMENTS

We thank L. Börjesson, S. Eriksson, M. Kakihana, J. M. Tarascon, and H. Wühl for the Zn-substituted samples. The experiments were performed at the Stanford Synchrotron Radiation Laboratory, which is supported by the U.S. Department of Energy, Office of Basic Sciences, and the National Institute of Health, Biotechnology Division. The work was supported in part by NSF Grants Nos. DMR-90-04325 and DMR-92-05204, and the Swedish Natural Science Research Council. This work was partially carried out on UC/National Laboratories PRT beam time.

[1]J. M. Tarascon, P. Barboux, P. F. Miceli, L. H. Greene, G. W. Hull, M. Eibschutz, and S. A. Sunshine, Phys. Rev. B **37**, 7458 (1988).

[2]Y. Maeno, M. Kato, Y. Aoki, and T. Fujita, Jpn. J. Appl. Phys. **26**, L1982 (1987).

[3]G. Xiao *et al.*, Phys. Rev. B **35**, 8782 (1987).

[4]J. M. Tarascon, L. H. Greene, B. G. Bagley, W. R. McKinnon, P. Barboux, and G. W. Hull, in *Novel Superconductivity*, edited by S. A. Wold and V. Z. Kresin (Plenum, New York, 1987), p. 705.

[5]Y. Maeno, T. Tomita, M. Kyogoku, S. Awaji, Y. Aoki, K. Hoshino, A. Minami, and T. Fujita, Nature **328**, 312 (1987).

[6]T. Kajtiani *et al.*, Jpn. J. Appl. Phys. **27**, L354 (1988).

[7]H. Maeda *et al.*, Physica C **157**, 483 (1989).

[8]G. Roth, P. Adelmann, R. Ahrens, B. Blank, H. Borkle, F. Gompf, G. Heger, M. Herview, M. Nindel, B. Obst, J. Pannetier, B. Renker, H. Rietschel, B. Rudolf, and H. Wuhl, Physica C **162-164**, 518 (1989).

[9]B. Jayaram, S. K. Agarwal, C. V. Narasimha Rao, and A. V. Narlikar, Phys. Rev. B **38**, 2903 (1988).

[10]R. S. Howland, T. H. Geballe, S. S. Laderman, A. Fischer-Colbrie, M. Scott, J. M. Tarascon, and P. Barboux, Phys. Rev. B **39**, 9017 (1989).

[11]M. Affronte, D. Pavuna, O. Martin, F. Lucci, T. Besagni, and S. Cattani, Solid State Commun. **70**, 951 (1989).

[12]P. F. Rajam, C. K. Subramaniam, S. Kasivswanathan, and R. Srinivasan, Solid State Commun. **71**, 475 (1989).

[13]K. Westerholt, H. J. Wuller, H. Bach, and P. Stauche, Phys. Rev. B **39**, 11 680 (1989).

[14]M. Kakihana, L. Borjesson, and S. G. Eriksson, Physica C **162**, 1251 (1989).

[15]S. Kim, R. A. Fisher, N. E. Phillips, and J. E. Gordon, Physica C **162**, 494 (1989).

[16]J. W. Loram, K. A. Mirza, and P. F. Freeman, Physica C **171**,

243 (1990).
[17]H. Shaked, J. Faber, Jr., B. W. Veal, R. L. Hiterman, and A. P. Paulikas, Solid State Commun. **75**, 445 (1990).
[18]N. C. Mishra, A. K. Rajarajan, K. Patnail, R. Vijayaraghavan, and L. C. Gupta, Solid State Commun. **75**, 987 (1990).
[19]Y. Zhu, M. Suenaga, and Y. Xu, J. Mater. Res. **5**, 1380 (1990).
[20]Y. Xu, R. L. Sabatini, A. R. Moddenbaugh, Y. Zhu, S.-G. Shyu, and M. Suenaga, Physica C **169**, 205 (1990).
[21]S. T. Ting, Y. Gao, C. S. Jee, S. Rahman, J. E. Crow, T. Mihalisin, G. H. Myer, I. Perez, R. E. Solomon, P. Schlottmann, and J. Schwegler, Physica C **163**, 227 (1990).
[22]B. Roughani, L. C. Sengupta, J. L. Aubel, S. Sundaram, and W. C. H. Joiner, Physica C **171**, 77 (1990).
[23]Q. Song, B. P. Clayman, and S. Gygax, Physica C **165**, 328 (1990).
[24]C. Tome-Rosa, G. Jakob, M. Maul, A. Walkenhorst, M. Schmitt, P. Wagner, P. Prsyslupski, and H. Adrian, Physica C **171**, 231 (1990).
[25]F. Bridges, J. B. Boyce, T. Claeson, T. H. Geballe, and J. M. Tarascon, Phys. Rev. B **39**, 11 603 (1989); **42**, 2137 (1990).
[26]M. Kakihana, L. Borjesson, E. Eriksson, P. Svedlindh, and P. Norling, Physica C **162**, 931 (1989).
[27]J. B. Boyce, F. Bridges, T. Claeson, and M. Nygren, Phys. Rev. B **39**, 6555 (1989), and references therein.
[28]J. G. Huber, W. J. Liverman, Y. Xu, and A. R. Moodenbaugh, Phys. Rev. B **41**, 8757 (1990).
[29]P. Carretta, M. Corti, A. Rigamonti, R. De Renzi, F. Licci, C. Paris, L. Bonoldi, M. Sparpaglione, and L. Zini, Physica C **191**, 97 (1992).
[30]H. Yamagata, K. Inada, and M. Matsumura, Physica C **185-189**, 1101 (1991).
[31]R. Kubiak and K. Westerholt, Physica C **173**, 232 (1991).
[32]P. Fournier, R. Gagnon, and M. Aubin, Physica C **177**, 159 (1991).
[33]W. Sadowsi, M. Affronte, M. Francois, and E. Walker, Physica C **185-189**, 453 (1991).
[34]K. Isida, Y. Kitaoka, T. Yositomi, N. Ogata, T. Kamino, and K. Asayama, Physica C **179**, 29 (1991).
[35]C. Y. Yang, A. R. Moodenbaugh, Y. L. Wang, Youwen Xu, S. M. Heald, D. O. Welch, M. Suenaga, D. A. Fischer, and J. E. Penner-Hahn, Phys. Rev. B **42**, 2231 (1990).
[36]H. Alloul, T. Ohno, H. Casalta, J. F. Marucco, P. Mendels, J. Arabski, G. Collin, and M. Mehbod, Physica C **171**, 419 (1990); P. Mendels, H. Alloul, J. F. Marucco, and G. Collin, *ibid.*, **171**, 429 (1990).
[37]I. Felner and B. Brosch, Phys. Rev. B **43**, 10 364 (1991).
[38]T. Miyatake, K. Yamaguchi, T. Takata, N. Koshizuka, and S. Tanaka, Phys. Rev. B **44**, 10 139 (1991).
[39]M. G. Smith, R. D. Taylor, and H. Oesterreicher, Phys. Rev. B **42**, 4202 (1990).
[40]Z. Q. Qui, Y. W. Du, H. Tang, and J. C. Walker, J. Appl. Phys. **67**, 5458 (1990).
[41]G. G. Li, F. Bridges, J. B. Boyce, and W. H. C. Joiner, Phys. Rev. B **47**, 12 110 (1993).
[42]R. Dupree, A. Gencten, and D. McK. Paul, Physica C **193**, 81 (1992).
[43]K. Ishida, Y. Kitaoka, N. Ogata, T. Kamino, and K. Asayama, Physica C **185-189**, 1115 (1991).
[44]Y. Zhao, H. K. Liu, J. R. Li, G. Yang, and S. X. Dou, Physica C **185-189**, 753 (1991).
[45]L. Albanese, C. Bucci, P. Carretta, R. De Renzi, G. Guidi, R. Tedeschi, F. Licci, C. Paris, G. Calestani, M. G. Francesconi, S. F. J. Cox, and C. A. Scott, J. Magn. Magn. Mater. **104-107**, 509 (1992).
[46]Y. C. Jean, C. S. Sundar, A. Bharathi, J. Kyle, H. Nakanishi, P. K. Tseng, P. H. Hor, R. L. Meng, Z. J. Huang, C. W. Chu, E. E. Wang, P. E. A. Turchi, R. H. Howell, A. L. Wachs, and M. J. Fluss, Phys. Rev. Lett. **64**, 1593 (1990).
[47]J. L. Routbort, S. J. Rothman, N. Chen, J. N. Mundy, and J. E. Baker, Phys. Rev. B **43**, 5489 (1991).
[48]R. Gajic, J. Schützmann, J. Betz, T. Zetterer, H. H. Otto, P. E. Obermayer, and K. F. Renk, Solid State Commun. **78**, 65 (1991).
[49]H. Alloul, P. Mendels, H. Casalta, J. F. Marucco, and J. Arabski, Phys. Rev. Lett. **67**, 3140 (1991).
[50]Y. Nakazawa, J. Takeya, and M. I. Shikawa, Physica C **174**, 155 (1991).
[51]A. I. Akimento, G. Goll, I. K. Yanson, H. v. Lohneysen, R. Ahrens, T. Wolf, and H. Wuhl, Condens. Matter **82**, 5 (1991).
[52]J. C. Phillips, Solid State Commun. **81**, 497 (1992).
[53]J. C. Phillips, Solid State Commun. **80**, 59 (1991).
[54]J. C. Phillips, Phys. Rev. Lett. **64**, 1605 (1990).
[55]J. C. Phillips, Phys. Rev. B **41**, 8968 (1990).
[56]F. Bridges, G. Li, J. B. Boyce, and T. Claeson, Proc. SPIE **1550**, 76 (1991).
[57]T. Claeson (private communication).
[58]T. M. Hayes and J. B. Boyce, in *Solid State Physics,* edited by H. Ehrenreich, F. Seitz, and D. Turnbull (Academic, New York, 1982), Vol. 37, p. 173.
[59]G. G. Li, F. Bridges, and G. Brown, Phys. Rev. Lett. **68**, 1609 (1992).
[60]J. Mustre de Leon, J. J. Rehr, S. I. Zabinsky, and R. C. Albers, Phys. Rev. B **44**, 4146 (1991).
[61]J. B. Boyce, F. G. Bridges, T. Claeson, T. H. Geballe, G. G. Li, and A. W. Sleight, Phys. Rev. B **44**, 6961 (1991).
[62]H. Renevier, J. L. Hodeau, and M. Marezio, in *Lattice Effects in High-T_c Superconductors,* edited by Y. Bar-Yam, T. Egami, J. Mustre-de Leon, and A. R. Bishop (World Scientific, New Jersey, 1992), p. 118.